Friction

Research Article

Suppressed friction-induced temperature rise at energetic β-HMX crystal interfaces by wax coating

Hongtu He[1,✉], Guocheng Li[1,2], Xiao Zhu[1], Huijing Duan[1], Jiaxin Yu[1], Rui Liu[3], Yanyang Qu[2], Ying Yin[2,✉]

Cite this article: He HT, Li GC, Zhu X, et al. *Friction* 2025, **13**(12): 9441063. https://doi.org/10.26599/FRICT.2025.9441063

ABSTRACT: Modifying the surface properties of energetic materials with coating has theoretical and practical significance in the field of their application. Wax, in its role as a functional lubrication layer, has extensive utility in mitigating the sensitivity of explosives to external stimuli. This study aims to investigate the friction behavior and temperature rise of β-octahydro-1,3,5,7-tetranitro-1,3,5,7-tetrazocine (β-cyclotetramethylenetetranitramine, or β-HMX) crystals with and without the wax coating, and the friction coefficient, frictional temperature rise, and frictional work-heat conversion rate were systematically analyzed. The experimental results show that regardless of single and reciprocating scratch conditions, the wax coating significantly reduced the coefficient of friction of the β-HMX surface by up to 63% and effectively suppressed the temperature rise during friction by up to 83%. Further analyses reveal that under single scratch conditions, the frictional work-heat conversion rate of the pristine β-HMX surface is approximately 42%, whereas that of the wax-coated surface increases to about 30% with the frictional power density, which involves the contact pressure, sliding speed, and friction coefficient. In contrast, under reciprocating scratch conditions, the frictional work-heat conversion rate of the uncoated β-HMX surface decreases with increasing number of sliding cycles, which is related to the increase in surface temperature and potential surface damage. The frictional work-heat conversion rate of wax-coated surfaces increases with increasing number of sliding cycles until the contact pressure is high enough that the lubricating effect of the wax layer diminish and the conversion rate begin to decrease. The obtained results not only pave the way for understanding the friction energy regulation and desensitization mechanism of wax on the surface of energetic crystals at the micro and quantitative levels but also provide a necessary basis for establishing friction hotspot models under dry friction and wax lubrication conditions from the aspects of friction characteristic parameters, frictional temperature rise, and the work-heat conversion rate.

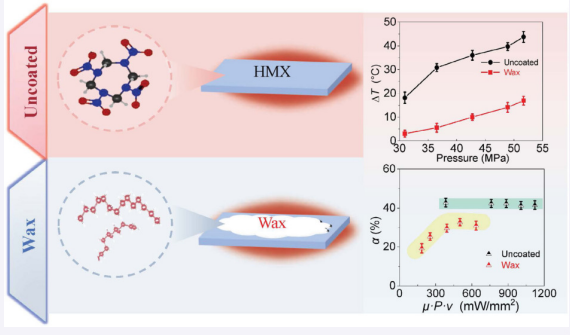

KEYWORDS: energetic crystal; β-octahydro-1,3,5,7-tetranitro-1,3,5,7-tetrazocine (β-cyclotetramethylenetetranitramine; β-HMX); friction; coating; temperature rise

1 Introduction

As a typical representative of energetic materials (EMs), β-octahydro-1,3,5,7-tetranitro-1,3,5,7-tetrazocine (β-cyclotetramethylenetetranitramine, or β-HMX) has attracted great attention because of its superior energetic performance and is widely applied in plastic bonded explosives (PBXs), solid rocket propellants, civil civilian explosives, etc. [1–3]. The superior energy properties of EMs not only facilitate efficient destruction but also introduce safety concerns during their manufacturing and usage [4], which may lead to significant casualties, military equipment failures, and economic losses. Friction interaction at the surface and interface of EMs is a key mechanism that poses safety risks in explosives and involves pressing, polishing, finishing, cutting, and usage during infiltration and drop processes [5–7]. For instance, during the grinding process of energetic materials, the materials face frictional shear forces with the grinding tools, which can easily lead to fragmentation, large-scale deformation, and even accidental ignition of the energetic materials, thereby directly affecting their safety [8]. In the granulation process of energetic materials, the friction between the stirring rod and energetic material particles may cause a frictional temperature rise at the interface of the energetic particles, posing certain safety hazards [9]. In addition, during the transportation

[1] Key Laboratory of Testing Technology for Manufacturing Process in Ministry of Education, Southwest University of Science and Technology, Mianyang 621010, China. [2] Institute of Chemical Materials, China Academy of Engineering Physics, Mianyang 621999, China. [3] State Key Laboratory of Explosion Science and Technology, Beijing Institute of Technology, Beijing 100081, China.

✉ Corresponding authors. E-mail: H. He, hehongtu@swust.edu.cn; Y. Yin, yinying@caep.cn

Received: July 15, 2024; Revised: December 9, 2024; Accepted: December 27, 2024

and use of energetic materials, special attentions should be given to the risks of friction hotspots and even ignitions caused by accidental stimuli such as accidental drops and impacts [10]. Once the friction-induced temperature rise reaches a critical threshold, violent reactions or even the ignition of EMs can occur [11]. Thus, it is of great importance to gain insight into the friction properties of EMs and explore methods to control both the frictional temperature rise and their safety performance.

To date, numerous efforts have been made to improve the safety performance of EMs under mechanical stimulus, such as reducing internal defects [12] and surface roughness [13], as well as the sphericalization of EMs [14] and surface modification [15]. As a simple and easy way to improve mechanical sensitivity, coating treatment has been widely used to modify the surface of EMs. For instance, wax [16], graphite [17], stearic acid [18], carbon nanomaterials [19], and polymers [20] have been reported to reduce the friction sensitivity of explosives. However, it should be noted that the friction sensitivity of EMs is essentially a statistical probability, and its underlying mechanism remains unclear [4]. While surface coating treatments are known to alter the friction coefficient and wear behavior of solid materials [21, 22], the precise mechanism by which surface coatings affect friction and the corresponding temperature rise at the EMs interface is still poorly understood.

In addition, another important issue of the traditional friction sensitivity of EMs is that such measurements are based on micro/nanoscale particles with a given mass (e.g., 20 mg), which complicates a thorough comprehension of the friction mechanisms at the EM interface. To overcome this, it is particularly important to carry out quantitative friction analysis directly toward the interface of energetic crystals. Recently, when a diamond tip was rubbed via nanoscratch tests, the friction coefficient of β-HMX crystals, one of the most widely used energetic crystals in the modern military industry, varied with the applied pressure, scratch direction, and crystal planes [23]. Furthermore, in the presence of a 2 μm thick wax coating on the β-HMX surface, the average friction coefficient on the β-HMX surface decreased to ~0.2 compared with that on the uncoated surface under the same tribological conditions [24]. The fluctuation or anisotropy of the friction coefficient of the β-HMX surface was also reduced by the wax coating. Note that the counter-surface used in the nanoscratch was a rigid diamond tip with a high thermal conductivity of 22 W/(cm·K) [25] compared with that of β-HMX (~0.4 W/(cm·K)) [26], and the sliding speed was relatively slow (in the range of μm/s). This can lead to a very limited temperature rise, making on-site measurement of temperature rise extremely difficult. Moreover, since friction interactions between energetic crystals play a critical role in the temperature rise [27], several important questions arise regarding the friction sensitivity or safety of energetic β-HMX surfaces: (1) How does wax coating treatment alter the friction coefficient of the β-HMX surface when it is rubbed with the β-HMX surface itself? (2) How does the wax coating affect the temperature rise at β-HMX interfaces?

To address these challenges, this study conducted an in-depth investigation into the impact of wax coatings on the frictional behavior of β-HMX crystals and conducted a systematic analysis from the perspective of friction, revealing the role of wax coatings in this process. The effects of nominal pressure on the β-HMX interface upon single scratching and reciprocating scratching were studied, and the mechanisms of the friction coefficient, frictional temperature rise, frictional work-heat conversion rate, and friction sensitivity of β-HMX were investigated. The findings obtained can provide critical information on the frictional safety of β-HMX crystal surfaces, and their implications can be extended to other EMs.

2 Materials and methods

The β-HMX single crystals used as the substrate and counter-surface (upper friction pair) in the experiments were provided by the Institute of Chemical Materials, Chinese Academy of Engineering Physics, China. The basic crystal data of β-HMX can be found in a previous publication [23]. To prevent the underlying energetic HMX crystal (substrate) from shifting during the friction process, owing to the fragility of the HMX crystal, it is challenging to directly grip it with a metal fixture. To prepare the samples for the tribological tests, both the β-HMX single-crystal substrate and counter-surface were wrapped with cold inlay material (Meijun Technology Inspection Co., Ltd., China), and the curing process of the cold inlay material took place at room temperature, thereby avoiding crystal damage caused by thermal effects [24]. The samples were then embedded and polished via a grinding machine (ZYP230, McCord Material Processing Equipment Company, China). Wax particles were used as the lubricating material, and the preparation process of the coating involved melting the solid lubricant coating into a liquid state via a heating platform (P-20A, Guangzhou Huanghua Electronic Equipment Co., Ltd., China) at a temperature of 60 °C. Then, the melting lubricant was applied to the β-HMX single crystals before they cooled to room temperature (Fig. 1(a)). Using optical profilometry mounted on a universal tribometer (MFT300, Rtec, USA), the surface roughness S_a of the wax-coated surface was estimated to be 23.6±0.6 nm. The coating thickness was determined from the step edge of the coating after partial removal of the coating on the surface, as shown in Fig. 1(b). The thickness of the wax coating was estimated to be 2.5±0.2 μm (Fig. 1(c)). Uncoated β-HMX and wax-coated β-HMX are referred to as "uncoated" and "wax" for simplicity, respectively, hereafter.

Tribological experiments on the β-HMX surface were performed with a universal tribometer (MFT300, Rtec, USA). The counter-surface was β-HMX with a cylindrical shape and was 1 mm in diameter and 4 mm in height. Since the wear or damage of both the counter-surface and substrate may occur during the

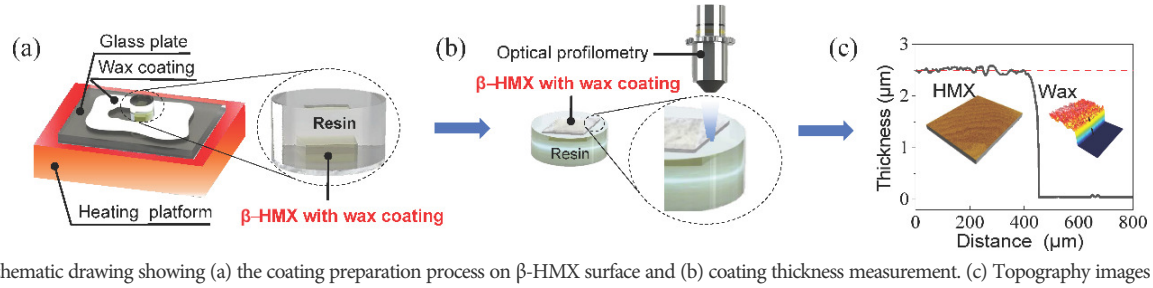

Fig. 1 Schematic drawing showing (a) the coating preparation process on β-HMX surface and (b) coating thickness measurement. (c) Topography images and cross-sectional line profile showing coating surface roughness and thickness of coatings on β-HMX surface.

friction process, which may alter the accurate contact area, the nominal contact pressure was used in the present study. The initial contact pressure was set from ~30 to ~65 MPa, the sliding speed was 50 mm/s, and the sliding distance was 15 mm. To ensure the reliability of the experimental data, at least five tribological experiments under each condition were performed, and only the mean value and standard error were shown in this paper. The room temperature and relative humidity (RH) were 20 °C and 50%, respectively.

The frictional temperature at the β-HMX interface was analyzed in-situ by a fast infrared (IR) camera (Fast M200, Canada), which was mounted in the upper front of the tribometer for real-time monitoring of temperature changes at the friction interface. The thermal emissivity of β-HMX varied from 40% to 33%, and 35% of the thermal emissivity of β-HMX was selected; the relative error of the measured temperature remained relatively low (< 5%), as shown in Fig. S1 in the Electronic Supplementary Material (ESM). In the present study, the β-HMX substrate was located ~440 mm away from the lens, and the focal length of the IR lens was 50 mm, resulting in a magnification factor of 1.2 and a resolution of 120 μm. The time resolution of the IR camera was 5 ms, and its spatial resolution was 15 μm. The inherent accuracy error of the high-speed infrared thermometer was 1%.

To reveal the friction mechanism of β-HMX, surface damage to β-HMX was analyzed with an optical microscopy (BX51-P, Olympus, Japan), and the chemical structures of the wear debris, scratched region, and pristine β-HMX surface were detected via Raman spectroscopy (InVia, Renishaw, England). The friction sensitivity of the uncoated and wax-coated surfaces was determined with a BM-B pendulum friction apparatus (China Ordnance Industry 204 Research Institute, China), which was based on the GJB 5891.24-2006 standard method. 20 mg samples were placed between steel anvils and hit by a pendulum hammer fixed with a 66° tilt angle, and the gauge pressure was 1.5 MPa. Friction-induced ignition or explosion was defined as any evidence of flash, flame, or explosion that occurred during friction sensitivity measurements. Fifty samples were tested, and the explosion probability (P) was used to represent the friction sensitivity of the tested samples, where a greater P corresponded to a greater friction sensitivity of the tested sample.

3 Results and discussion

3.1 Suppressed friction coefficient and temperature rise at β-HMX interface upon single scratch

Figure 2(a) shows the friction coefficient on the uncoated and wax-coated β-HMX surfaces as a function of sliding time. Clearly, the friction coefficient of the coated β-HMX surface is much lower than that of the uncoated β-HMX surface. To compare the friction coefficients of the β-HMX surfaces under various conditions quantitatively, Fig. 2(c) shows the friction coefficient of

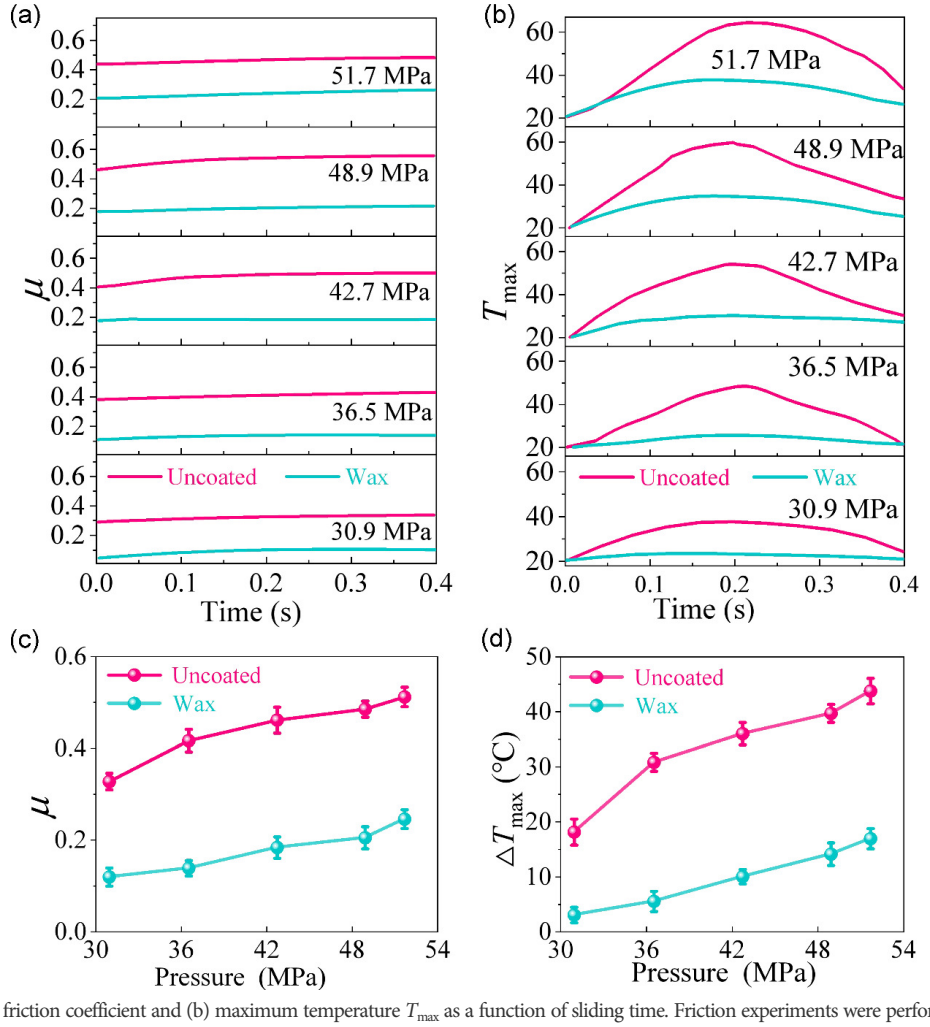

Fig. 2 Variations in (a) friction coefficient and (b) maximum temperature T_{max} as a function of sliding time. Friction experiments were performed with various initial contact pressures and a sliding speed of 50 mm/s. Sliding distance was 15 mm. (c) Friction coefficient and (d) temperature rise as a function of contact pressure.

the β-HMX surface under various coating conditions as a function of nominal contact pressure. As the nominal contact pressure increases from ~30.9 to ~51.7 MPa, the steady-state friction coefficient on the uncoated β-HMX surface increases from ~0.32 to ~0.51, while that on the wax-coated β-HMX surface increases from ~0.12 to ~0.26. These findings clearly show that the wax coating can significantly reduce the friction coefficient of the β-HMX surface by ~49%–63%.

Figure 2(b) shows the maximum temperature on the uncoated and wax-coated β-HMX surfaces as a function of sliding time. Similar to the friction coefficient, the maximum temperatures on the wax-coated β-HMX surface are much lower than those on the uncoated β-HMX surface. Notably, during a single scratch process, there are peak temperatures under various sliding contact conditions. This is because there is an acceleration and deceleration process of the sample stage to accomplish the single scratch process under the given sliding contact conditions. The sliding speed and acceleration process as a function of sliding time can be found in Fig. 3(a). When the speed increases to the set value, the friction speed reaches a constant value. The friction work is calculated every 50 ms as a stage. The friction work increases and then gradually stabilizes (Fig. 3(a)). The continuous accumulation of heat leads to a continuous increase in temperature. However, as the friction process progresses, the speed and friction work gradually decrease (Fig. 3(b)), thereby reducing the heat generated by friction. In addition, at this time, the temperature difference between the frictional temperature and the ambient temperature is large, and the heat loss also increases [28, 29], resulting in a decrease in temperature rise. To quantitatively compare the maximum temperature on the β-HMX surfaces under various conditions, Fig. 2(d) shows the maximum frictional temperature rise of the β-HMX surface under various coating conditions as a function of the nominal contact pressure. As the nominal contact pressure increases from ~30.9 to ~51.7 MPa, the maximum temperature rise on the uncoated *β*-HMX surface increases from ~18 to ~43.7 °C, while that on the wax-coated β-HMX surface increases from ~3 to ~16.9 °C. Clearly, the wax coating significantly reduces the maximum temperature rise on the β-HMX surface by ~61%–83%.

3.2 Suppressed friction coefficient and temperature rise at β-HMX interface upon reciprocating scratch

In addition to the single scratch, the reciprocating scratch on the β-HMX surface also represents a typical friction state in practical engineering applications [30]. In our previous research, the friction coefficient and corresponding temperature rise between β-HMX crystals significantly increase only when the contact pressure approaches ~20 MPa [31]. To more clearly elucidate the improvement effect of the lubrication interface on friction characteristics, contact pressures of ~18, ~27, and ~62 MPa are selected as typical contact pressure conditions in the present study. These conditions allow us to study the friction behavior and temperature responses of various friction interfaces under relatively low, medium, and high contact pressure conditions.

To assess and compare the impact of the uncoated and wax coatings on the friction coefficient and temperature rise on the β-HMX surface upon reciprocating scratching, Fig. 4 shows the friction coefficient and maximum temperature on the β-HMX surface as a function of sliding time or number of cycles under low, medium, and high contact pressure conditions. Under a relatively low contact pressure of ~18 MPa, the friction coefficients on the uncoated and wax surfaces remain stable at ~0.43 and ~0.17, respectively (Fig. 4(a)). This finding indicates that the wax coating can reduce the friction coefficient by ~60%. Similar to the single scratch conditions, it seems that there is a peak temperature in the single scratch direction. Thus, two peak temperatures can be found during one tribological cycle (Fig. 4(b)). To compare the temperature variation on the β-HMX surface per sliding cycle, the frictional temperature rise ΔT is calculated as the difference between the lowest and highest temperature during each sliding cycle, as shown in Fig. 4(c). The initial temperature rise on the uncoated β-HMX surface is ~15.2 °C, while it gradually decreases to ~8 °C as the number of sliding cycles increases to 10 (Fig. 4(c)). In contrast, when the β-HMX surface is coated with wax, the temperature rise is not decreased with increasing number of sliding cycles; instead, it increases with increasing number of sliding cycles, and the temperature rise increases from ~3.7 to ~5 °C (Fig. 4(c)). Under the given contact pressure and number of sliding cycles, the total temperature rise is ~40.2 and ~22.9 °C for the uncoated and wax surfaces, respectively (Fig. 4(b)). Notably, the wax surface represents the wax-coated β-HMX surface (Fig. 1(c)).

Under a relatively moderate contact pressure of ~27 MPa, the friction coefficient on the uncoated surface is ~0.52, and it slightly varies with sliding time. Although the friction coefficient on the wax surface is lower than that on the uncoated surface, it increases from ~0.18 to ~0.37 as the sliding time increases (Fig. 4(d)), which is different from that under low contact pressure conditions (Fig. 4(a)). The initial temperature rise on the uncoated β-HMX surface was ~25.4 °C, whereas it gradually decreased to ~9.4 °C as

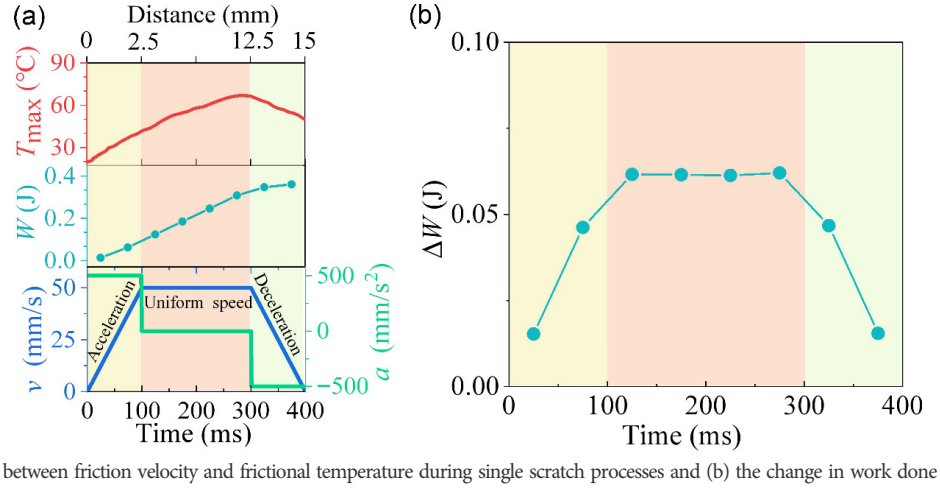

Fig. 3 (a) Relationship between friction velocity and frictional temperature during single scratch processes and (b) the change in work done during a single friction process.

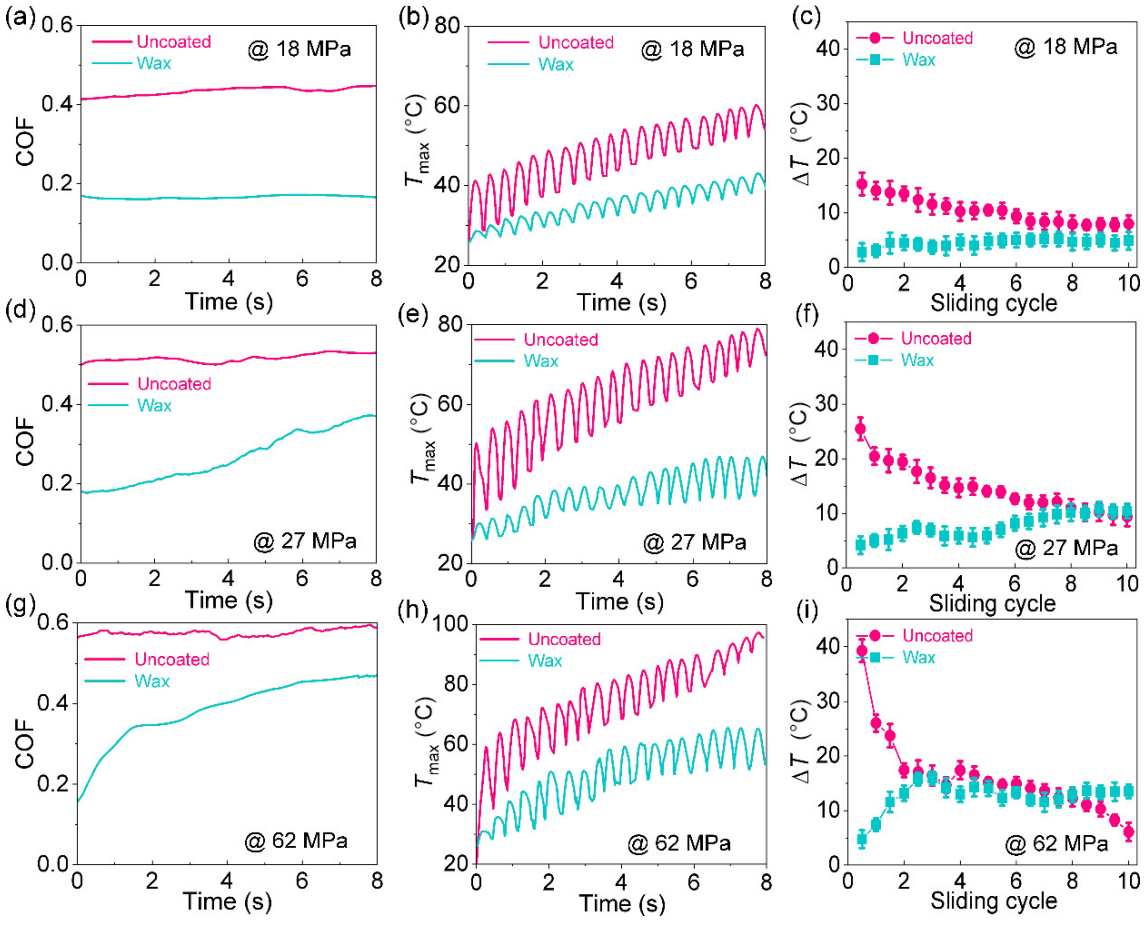

Fig. 4 Variations in (a, d, g) friction coefficient, (b, e, h) maximum temperature T_{max}, and (c, f, i) temperature rise ΔT as a function of the sliding time or number of cycles. Friction experiments were performed with initial contact pressures of (a–c) ~18 MPa, (d–f) ~27 MPa, (g–i) ~62 MPa and a sliding speed of 50 mm/s. The sliding distance was 15 mm.

the number of sliding cycles increased to 10 (Fig. 4(e)). When the β-HMX surface is coated with wax, the temperature rise increases from ~4 to ~10.4 °C (Fig. 4(f)). Under the given contact pressure and number of sliding cycles, the total temperature rise is ~58.8 and ~26.4 °C for the uncoated and wax surfaces, respectively (Fig. 4(e)).

As the nominal contact pressure increases to ~62 MPa, the friction coefficient on the uncoated surface increases to ~0.57 (Fig. 4(g)). Similar to the case of medium contact pressure, the friction coefficient on the wax surface increases from ~0.17 to ~0.44 as the sliding time increases (Fig. 4(g)). The initial temperature rise on the uncoated β-HMX surface is ~39.2 °C, whereas it gradually decreased to ~6.1 °C as the number of sliding cycles increased to 10 (Fig. 4(i)). When the β-HMX surface is coated with wax, the temperature rise increases from ~4.7 to ~13.5 °C (Fig. 4(i)). Under the given contact pressure and number of sliding cycles, the total temperature rise is ~77.1 and ~45.6 °C for the uncoated and wax surfaces, respectively (Fig. 4(h)).

The results in Fig. 4 clearly show that both the friction coefficient and the temperature rise on the uncoated and coated β-HMX surfaces strongly depend on the nominal contact pressure under reciprocating scratch conditions, which is similar to the case of single scratch conditions. The discrepancy between the single scratch and reciprocating scratch conditions is that the friction coefficients with sliding time under single scratch conditions are relatively stable (Fig. 2(a)), suggesting that one type of friction mechanism dominates the friction process. However, under reciprocating scratch conditions, the friction coefficient of the wax surface significantly varies with sliding time under medium and high contact pressure conditions (Figs. 4(d) and 4(g)), suggesting that the counter-surface may penetrate the coating to the β-HMX surface under certain conditions and thus alter the friction behavior [24].

To verify this, Fig. 5 shows the Raman spectra of the scratched region and debris from the uncoated and coated β-HMX surfaces. The four main Raman features of the pristine β-HMX surface are found at ~834, ~882, ~951, and ~1,312 cm^{-1}, which can be assigned to the C-N bond, N-N bond, HMX ring, and $-NO_2$ bond in the β-HMX crystal, respectively [32, 33]. Regardless of various contact pressure conditions, no discrepancy is found in the scratched region and debris of the uncoated surface (Figs. 5(a), 5(b), and 5(c)), indicating that no tribochemical reactions occur under the given sliding contact conditions and that mechanical interactions such as plowing and peeling are the dominant mechanism during the friction process [23]. In the case of the wax-coated surfaces, there is only one Raman feature at ~2,963 cm^{-1} on the pristine wax surface (Fig. 5(d)), which can be assigned to CH_2 stretching of the wax [34]. Moreover, there is only one Raman feature of wax in the scratched region and debris under a low contact pressure of ~18 MPa, indicating that the counter-surface is only scratched with the wax coating and does not penetrate into the β-HMX. However, under a medium contact pressure of ~27 MPa and a high contact pressure of ~62 MPa, the Raman features of both wax and β-HMX can be found in the scratched

region and debris (Figs. 5(e) and 5(f)), indicating that the counter-surface is scratched with β-HMX under these conditions.

3.3 Suppressed frictional work-heat conversion rate at β-HMX interface

Generally, the frictional energy that puts into the sliding interface can be dissipated into wear or deformation and frictional heat [35, 36]. From the perspective of the friction safety of EMs, the friction-induced temperature at the EMs surface can be expressed as [24, 37]:

$$\frac{\partial}{\partial y}\left(-k\frac{\partial T}{\partial y}\right)+\rho\Delta HZ\exp\left(-\frac{E_A}{RT}\right)+\alpha\mu F\frac{\partial v_x}{\partial y}=\rho c\frac{\partial T}{\partial t} \quad (1)$$

where the first, second, and third terms represent the thermal conduction, heat by thermal decomposition, and total frictional energy (frictional work), respectively, whereas the right term represents the energy needed for the temperature rise; α is the frictional work-heat conversion rate; μ is the friction coefficient; F is the applied pressure, Pa or N·m^{-2}; v is the sliding speed, m·s^{-1}; ΔH is the explosion heat, J·kg^{-1}; Z is the preexponential factor, s^{-1}; E_A is the activation energy; R is the gas constant, J·(K·mol)$^{-1}$; T is the absolute temperature, K; c is the specific heat capacity, J·(kg·K)$^{-1}$; ρ is the material mass density, kg·m^{-3}; k is the thermal conductivity, W·(m·K)$^{-1}$.

The thermal decomposition term, the second term on the left side of Eq. (1), only starts to impact the temperature rise when the local temperature of HMX surpasses the thermal decomposition temperature (~220 °C) [38]. However, this was not achieved in this study, and the heat generated by thermal decomposition could be ignored. If we consider compensating for the heat lost due to heat transfer in the first item on the left, the relationship between the frictional work and heat required for actual temperature rise ΔT_a can be expressed as Eq. (2):

$$\alpha\mu F\frac{\partial v_x}{\partial y}=\rho c\frac{\partial T}{\partial t}+\frac{\partial}{\partial y}\left(k\frac{\partial T}{\partial y}\right) \quad (2)$$

The frictional work-heat conversion rate α can be expressed as Eq. (3):

$$\alpha=\left[\rho c\frac{\partial T}{\partial t}+\frac{\partial}{\partial y}\left(k\frac{\partial T}{\partial y}\right)\right]/\left(\mu F\frac{\partial v_x}{\partial y}\right) \quad (3)$$

This means that if the frictional heat loss by thermal conduction is well estimated, then the frictional work-heat conversion rate α can be estimated as the energy ratio between heat generation and frictional work under the given tribological conditions. If we assume that the temperature loss at the β-HMX surface as a function of time is independent of the tribological conditions, then the temperature loss $\Delta T'$ during the tribological process can be equal to that after the tribological process, and the latter can be measured in situ after the tribological process, as shown in Fig. S2 in the ESM. Consequently, the temperature loss measured in Fig. S2 in the ESM was compensated for on top of the original measured frictional temperature rise ΔT, and the actual frictional temperature rise ΔT_a at the β-HMX surface can be corrected, as shown in Fig. S3 in the ESM, i.e., the actual frictional temperature rise ΔT_a is equal to the sum of the measured frictional temperature rise ΔT and the temperature loss $\Delta T'$.

Theoretically, the temperature rise at the β-HMX surface upon a single scratch, i.e., the frictional work completely converts into frictional heat. Additionally, the physical effects of heat partitioning during the friction process must be considered. In the present study, the heat partitioning coefficient of theoretical frictional work is assumed to be 0.5 since the physical properties of the substrate and counter-surface are identical [39, 40]. Therefore, the theoretical temperature rise ΔT_t can be estimated by Eq. (4) [30]:

$$\Delta T_t=\frac{0.5\cdot P\cdot\mu\cdot v\cdot\varphi S\cdot t}{c\cdot\rho\cdot\varphi S\cdot\varphi H} \quad (4)$$

where P is the contact pressure; μ is the friction coefficient; v is the sliding speed; φS is the contact area per unit; t is the sliding contact time; c is the specific heat capacity; ρ is the density of the β-HMX crystal; φH is the depth per unit. The frictional work-heat

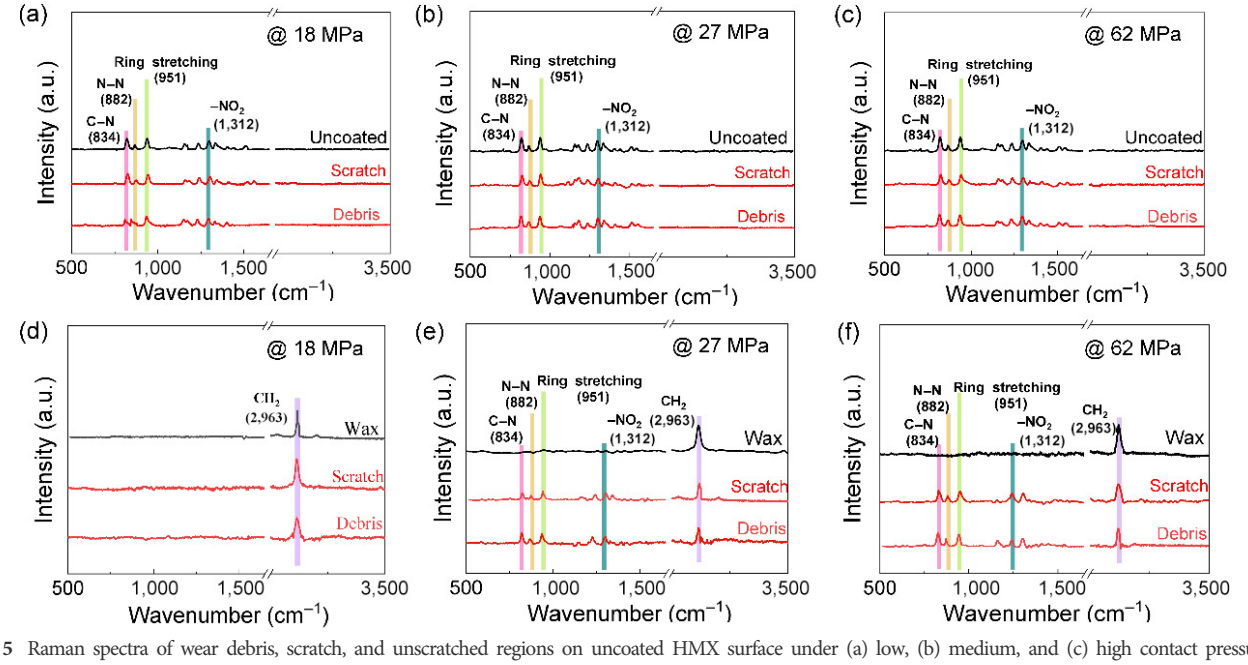

Fig. 5 Raman spectra of wear debris, scratch, and unscratched regions on uncoated HMX surface under (a) low, (b) medium, and (c) high contact pressures, respectively. Raman spectra of wear debris, scratch, and unscratched regions on wax-coated HMX surface under (d) low, (e) medium, and (f) high contact pressures, respectively.

conversion rate at the β-HMX interfaces upon a single scratch process can be subsequently estimated by the ratio between the actual temperature rise and the theoretically temperature rise. Equation (5) indicates that the frictional temperature rise ΔT is strongly dependent on the contact pressure (P), friction coefficient (μ), and sliding speed (v). Figure 7(a) compares the theoretical and actual temperature rise on β-HMX interfaces during a single frictional process as a function of the product of the contact pressure, friction coefficient and sliding speed, which represents the frictional power density [41]. The frictional temperature rise of the wax coating samples was consistently lower than that of the uncoated samples as the friction power density varied, confirming the effectiveness of the wax coating in suppressing the frictional temperature rise. Under the given sliding contact conditions during a single frictional process, the frictional work-heat conversion rate on the pristine β-HMX surface is ~42%, regardless of the friction power density (Fig. 7(b)). When coated with wax, the frictional work-heat conversion rate increases from ~19% to ~31% (Fig. 7(b)). As the power density increases, the temperature also increases. This reduces the viscosity of the wax material and requires less energy to overcome plastic deformation [27]. As a result, the heat generated by frictional work progressively increases, indicating that frictional heat is much lower than that of the uncoated surface.

In contrast to the single scratch process, the reciprocating scratch process may complicate energy consumption since the microfriction interface structure evolves over the course of the sliding cycle, as evidenced by the variation in the friction coefficient and temperature rise with increasing number of sliding cycles. The frictional work W_f that is input into the β-HMX substrate per unit area can be calculated by Eq. (5) [31]:

$$W_f = \frac{\int \mu F v \mathrm{d}t}{2} \tag{5}$$

where μ is the friction coefficient; F is the applied pressure; v is the nominal sliding speed; t is the sliding time. Here, the frictional work to the upper and lower materials is assumed to be the same; consequently, the average distribution of heat during frictional work can be estimated. In addition, the local heating, or per unit spatial dimension heating, of the β-HMX substrate caused by friction can be estimated as Eq. (6) [42]:

$$Q = \int_0^S \int_0^H c\rho \Delta T_a \mathrm{d}S\mathrm{d}H \tag{6}$$

where c is the specific heat capacity; ρ is the density of the β-HMX crystal; ΔT_a is the actual temperature rise; S is the contact area per unit; H is the depth per unit. Therefore, the frictional work-heat conversion rate α per unit scale of β-HMX crystal can be estimated as Eq. (7) [31]:

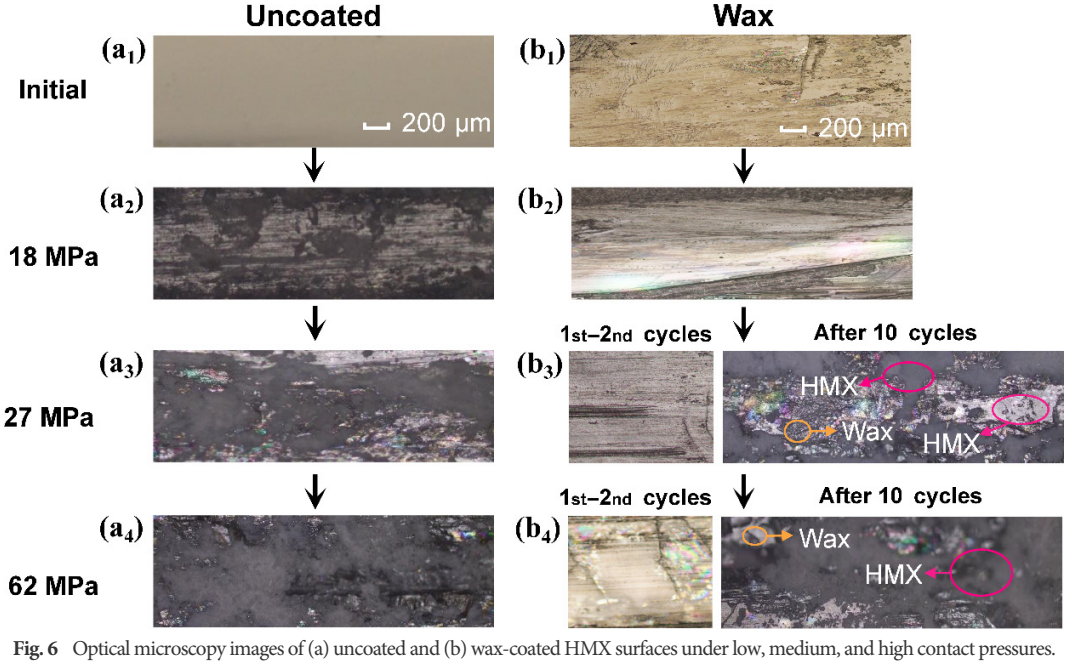

Fig. 6 Optical microscopy images of (a) uncoated and (b) wax-coated HMX surfaces under low, medium, and high contact pressures.

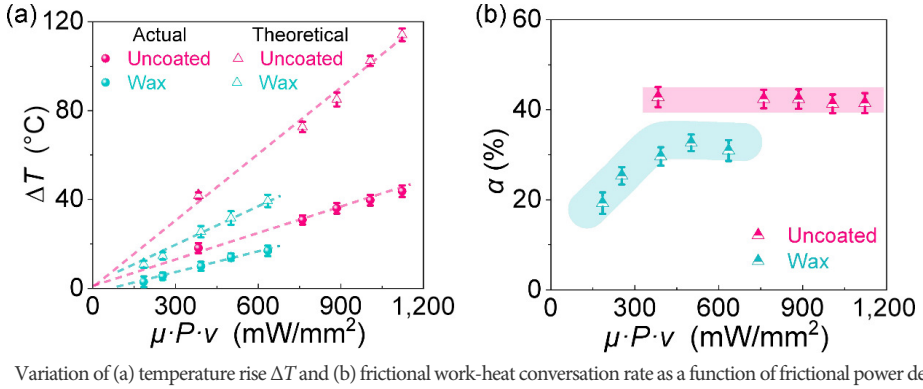

Fig. 7 Variation of (a) temperature rise ΔT and (b) frictional work-heat conversation rate as a function of frictional power density.

清華大学出版社 Tsinghua University Press | SciOpen

$$\alpha = \frac{Q}{W_f} \tag{7}$$

As shown in Fig. 8(a), under a nominal contact pressure of ~18 MPa, the frictional work-heat conversion rate α on the uncoated β-HMX surface decreases from ~46.3% to ~24.6% as the number of sliding cycles increases. Similarly, the α on the uncoated β-HMX surface decreases from ~45.8% to ~18.8% and from ~42.2% to ~12.7% under contact pressures of ~27 and ~62 MPa, respectively (Figs. 8(b) and 8(c)). The decrease in α on the uncoated β-HMX surface with increasing number of sliding cycles can be explained by the higher initial surface temperature of the uncoated β-HMX surface with increasing number of sliding cycles (Figs. 4(b), 4(e), and 4(h)), and the higher initial surface temperature is accompanied with the higher heat loss by thermal conduction under the same conditions; thus, the obtained heat decreases with increasing number of sliding cycles and thus decreases α. The increased surface damage or wear of the β-HMX surface with increasing number of sliding cycles may also contribute to the lower α since the increased surface damage or wear dissipates more energy [45, 46].

In contrast, when coated with wax, α increases with increasing number of sliding cycles. Under a contact pressure of ~18 MPa, the α of the wax-coated surface increases from ~24.2% to ~41.7% (Fig. 8(a)). Under a contact pressure of ~27 MPa, the α of the wax-coated surface increases from ~24.7% to ~29.8% (Fig. 8(b)). Under a contact pressure of ~62 MPa, the α of the wax-coated surface first increases from ~17.4% to ~27% and then decreases to ~14% (Fig. 8(c)). The initial work W_f can be dissipated mainly through plastic deformation, and the α of the wax-coated surface is much lower than that of the uncoated HMX surface, which is due to the friction interactions remaining at the wax layer and not at the HMX surface, indicating a good lubrication state with a relatively low COF (Fig. 4(a)). At this stage, the friction at the absorption point of the wax layer at the interface (denoted as W_1 in Fig. 9) significantly suppresses the frictional temperature rise ΔT (Fig. 4(c)). As the number of sliding cycles increases, the wax coatings provide excellent lubrication and protection, and under the protection of the wax layer, they can effectively prevent significant damage to the β-HMX crystal surface under low-contact pressure conditions (Figs. 6(a_2) and 6(b_2)). Because the friction interface is still in a good lubrication state with stable W_f (stable low COF), the amount of interface wax available for plastic deformation and heat absorption (W_1) is continuously reduced, which leads to an increase in ΔT per cycle (Fig. 4(c)), implying a greater Q and a higher α. Because stable lubrication that eventually results from reciprocating friction, α tends to stabilize at a high level.

In addition, as the contact stress increases to medium pressure (~27 MPa), the wax layer can protect the crystal surface during the first few friction cycles (Figs. 6(a_3) and 6(b_3)), but as the number of friction cycles increases, the crystal surface gradually deteriorates, and the friction process shifts to a mixed friction regime where lubrication and dry friction coexist. Apparently, the mixed friction effect can lead to greater frictional work W_f corresponding to a rising COF, along with a greater ΔT per cycle (Figs. 4(d)–4(f)), which contributes to a greater Q. Accordingly, the synchronous growth of W_f and Q could result in a relatively stable or slowly increasing α (Fig. 8(b)). Notably, α decreases over the last few cycles, which is possibly due to the severe brittle fracture of energetic crystals, which represents another form of dissipation for W_f (Fig. 6(b_3)).

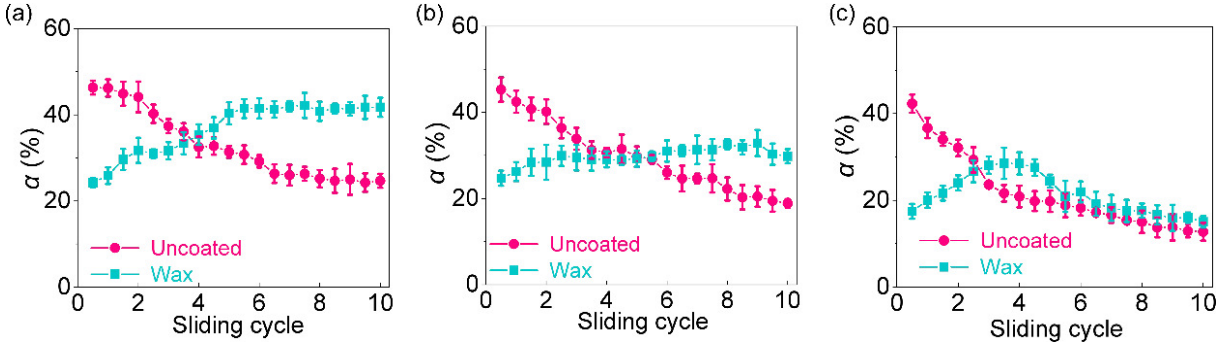

Fig. 8 Variation in frictional work-heat conversion rate as a function of number of sliding cycles under (a) low, (b) medium, and (c) high contact pressure conditions.

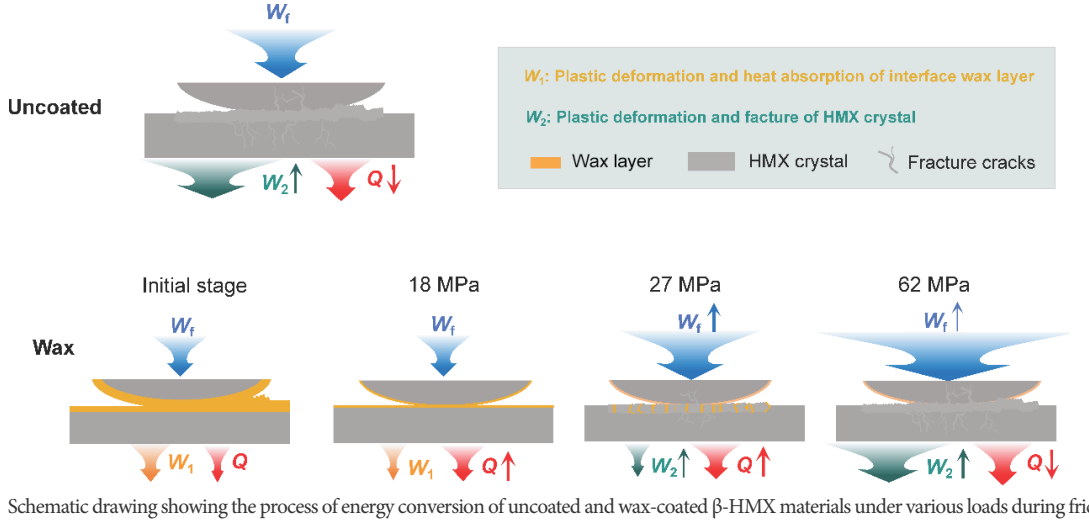

Fig. 9 Schematic drawing showing the process of energy conversion of uncoated and wax-coated β-HMX materials under various loads during friction.

Under high pressure (~62 MPa), the wax layer is more susceptible to damage during the first few rounds of friction, resulting in more severe damage and grain friction on the crystal surface during reciprocating friction (Figs. 6(a_4) and 6(b_4)), reflected in a rapidly increasing friction coefficient (from 0.17 to 0.45) and frictional temperature rise (Figs. 4(g)–4(i)), leading to an increase in α during the initial cycles. In the middle-to-late stages of reciprocating friction, severe crystal plasticity or brittle fracture (Fig. 6(b_4)) emerges as the primary mechanism (denoted as W_2 in Fig. 9) for energy dissipation, approaching dry friction. At this stage, ΔT per cycle stabilizes (Fig. 4(i)), yet the COF increases (Fig. 4(g)), suggesting that an increasing proportion of W_f is allocated to crystal deformation and damage (W_2), thereby resulting in a continuous decrease in α (Fig. 8(c)).

3.4 Suppressed frictional sensitivity of β-HMX by coating

Since the friction coefficient, frictional work-heat conversion rate, and temperature rise ΔT on the wax-coated surface are lower than those on the uncoated surface under the given tribological conditions (Figs. 2–9), it is reasonable to speculate that a similar reduction in friction properties at the wax surface could occur under extreme tribological conditions, such as friction-induced ignition behavior. To verify this, Fig. 10(b) compares the friction sensitivity of pristine and coated β-HMX. Under the given conditions, the friction sensitivity of pristine β-HMX is 72%, which is slightly lower than the previously reported value (100%) [43]. There are two possible reasons for this. First, the raw β-HMX used in the present study is high-quality β-HMX with fewer internal crystal defects; thus, the frictional sensitivity of β-HMX could be relatively lower [44]. Second, the tilt angle of the pendulum hammer and the gauge pressure applied as the sliding speed and normal force for the frictional sensitivity tests are relatively lower; thus, the obtained frictional sensitivity of the β-HMX could be relatively lower.

More importantly, when the β-HMX crystals is coated with wax, the frictional sensitivity is significantly decreased to 16% (Fig. 10(b)). This finding indicates that wax can significantly reduce the probability of friction-induced ignition or explosion. One may question whether frictional sensitivity reveals the probability of friction-induced ignition or explosion of EMs, and this determination of ignition or explosion is dependent on the subjective judgment of the experimenter via evidence of flash, flame or explosion; thus, frictional sensitivity is not a reliable and accurate parameter for understanding the role of a coating on the friction behavior of β-HMX. Nevertheless, the significant reduction in friction sensitivity caused by the wax coating indicates that the local temperature at the sliding interface is indeed suppressed by the presence of the wax coating.

During frictional sensitivity tests, the friction force comes from two sources: the friction between β-HMX and the sliding stainless steel surface and the friction between β-HMX particle grains [45]. The former friction occurs due to the sliding motion of the sliding pole (Fig. 2(a)), whereas the latter friction force makes the planes of grains slide with each other [46]. Recent simulation results revealed that the external friction heat between EMs and sliding columns had little effect on ignition, whereas the friction interactions between EMs themselves played a key role in ignition [27]. This is because the sliding column has a relatively high thermal conductivity that is detrimental to local heat or hot-spot formation in EMs [27]. If the friction between β-HMX particle grains dominated the temperature rise ΔT during the friction sensitivity tests, the suppressed friction coefficient, frictional work-heat conversion rate, and temperature rise ΔT caused by the wax coating (Figs. 2–9) could support the lower friction sensitivity since both the frictional work and frictional heat could be suppressed by the wax coating (Eq. (1)).

3.5 Frictional safety assessment of EMs beyond the temperature rise

Given the importance of safety concerns during manufacturing and usage, the friction sensitivity of Ems, which is based on statistical methods of friction ignition phenomena, has been widely used to assess safety by engineers. For example, if 10 ignition phenomena of crystal powder are observed in 20 tests under the same conditions, the friction sensitivity of the energetic crystal is recorded as 50%. Clearly, this statistical result lacks any physical information regarding the friction characteristics of EMs, and it does not provide any information on the response patterns of the friction temperature rise of EMs to the contact stress, friction coefficient, and so on. Frictional hot-spot theory has been widely used to analyze the friction safety of EMs, where friction interactions play a key role in the initial temperature rise, while the thermal decomposition plays a key role in the ignition of EMs once the local temperature exceeds the critical temperature of thermal decomposition [47, 48]. In the initial stage of the temperature rise ΔT, the frictional heat at the sliding interface is the only energy source. To simulate frictional hot spots on the EMs' surface, an appropriate value of the friction coefficient is important for determining frictional work (Eq. (1)). When the β-HMX surface is rubbed against the β-HMX surface, the friction coefficient at the β-HMX surface is not a fixed value but rather a dynamic parameter that depends on the nominal contact pressure (Figs. 2(a), 4(a), 4(d), and 4(g)) and sliding speed [33]. Previous investigations on the nanoscratch properties of the β-HMX surface upon a diamond tip revealed that the friction coefficient ranged from 0.2 to 0.7, depending on the contact pressure and sliding speed as well as the surface damage and crystallographic orientation [23]. However, in the simulation of the frictional heat

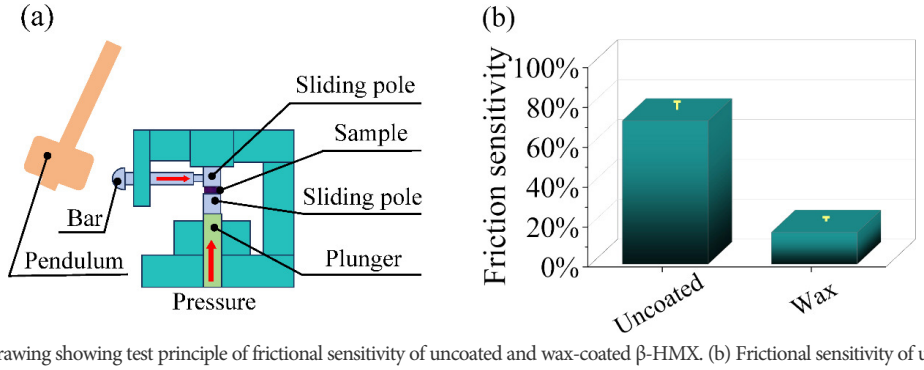

Fig. 10 (a) Schematic drawing showing test principle of frictional sensitivity of uncoated and wax-coated β-HMX. (b) Frictional sensitivity of uncoated and wax-coated β-HMX.

清華大学出版社 Tsinghua University Press | SciOpen

of EMs, a friction coefficient of 0.1–0.2 was used [49–51], which is not consistent with the experimental results. In addition to the friction coefficient, the frictional work-heat conversion rate is also a critical parameter for determining the friction-induced temperature rise ΔT of EMs (Eq. (1)). Moreover, previous numerical simulations of the ignition behavior of EMs considered the work-heat conversion rate to be stable (usually ~0.9) [52, 53]. However, the results in Figs. 7 and 8 clearly show that the frictional work-heat conversion rate is ⩽ 0.5 and could vary with the number of sliding cycles and counter-surface. The inconsistency of the friction coefficient and frictional work-heat conversion rate in simulations and experiments reveals that a more accurate value of the friction coefficient and frictional work-heat conversion rate is needed to determine the frictional heat and thus the friction-induced temperature rise ΔT of EMs, in addition to the applied normal pressure and sliding speed (Eq. (1)).

The findings obtained in the present study also reveal that the classic frictional parameter cannot be simply applied to the friction safety assessment of EMs. A nominal contact pressure is used in the typical friction sensitivity of EMs, or the critical pressure or pressure can be used to determine the frictional safety boundary of EMs under a given sliding speed [34]. These methods for ensuring the frictional safety of EMs cannot explain the dependence on both the contact pressure and the sliding speed well [54]. The friction power, which involves the friction force and sliding speed, is used to connect the temperature rise of the EMs [48]. Although the integration of friction power over time emphasizes the friction work at the EMs' interface and incorporates the friction coefficient, applied pressure, and sliding speed, the friction power at the EMs' interface cannot explain local ignition by friction or hot-spot formation [10]. More recently, the frictional power density, which is defined as the friction power per unit area, has been used to explain the frictional temperature rise on the EMs surface [33]. The use of frictional power density at the EM interface can also explain the hot-spot formation, which depends on the local contact area [55]. To simulate the local temperature rise of EMs under the given sliding contact conditions, the frictional power density and work-heat conversion rate can mimic more accurate frictional heat [55]. In addition to the direction connection between the frictional power density and temperature rise both below the critical point of thermal decomposition and close to the ignition temperature, the connection between the frictional power density and friction sensitivity in engineering applications can also be helpful for fully revealing the friction safety of EMs, which will be a research topic in future studies.

Moreover, compared with the uncoated β-HMX surface, the presence of a coating on the β-HMX surface can reduce the friction sensitivity (Fig. 10), friction coefficient (Figs. 2(a), 4(a), 4(d), and 4(g)), frictional temperature rise (Figs. 2(d), 4(c), 4(f), and 4(i)), and frictional work-heat conversion rate (Figs. 7(b) and 8). The reduced friction coefficient due to the presence of the coating on the β-HMX surface indicates that the friction power density also decreases; thus, the frictional work per unit area (μPv) on the coated surface is lower than that on the uncoated surface. Furthermore, the frictional work-heat conversion rate on the coated surface is lower (Figs. 7(b) and 8), along with the lower friction work per unit area on the coated surface, indicating that frictional heat is much lower than that on the uncoated surface and thus that the frictional temperature rise is lower (Figs. 2(d), 4(c), 4(f), and 4(i)).

Under reciprocating scratch conditions, the surface temperature on β-HMX increases with increasing sliding time or number of cycles (Figs. 4(b), 4(e), and 4(h)), implying that the initial surface temperature of β-HMX increases with increasing sliding time or number of cycles. The friction behavior and temperature rise on the subsequent friction cycles may affect the surface temperature generated during the previous friction cycles. This temperature effect on the friction behavior of β-HMX is different from the environmental temperature effect, since there is a local temperature rise on the β-HMX surface, and this temperature is increased by the heat accumulation effect caused by friction interactions in the present study, whereas the environmental temperature can heat entire EMs rather than locally temperature rise [4, 56]. How the environmental temperature affects the friction sensitivity and friction behavior as well as the temperature rise on EMs remains to be tested and will be one of our research topics in future studies.

4 Conclusions

In this study, the influence of wax coating on the tribological properties and temperature rise of β-octahydro-1,3,5,7-tetranitro-1,3,5,7-tetrazocine (β-cyclotetramethylenetetranitramine, or β-HMX) surfaces was investigated. The wax coating can significantly reduce the friction coefficient of β-HMX surfaces by as much as 49%–63% and effectively reduce the frictional temperature rise during friction by 61%–83%. This effect was particularly significant at medium and high contact pressures, not only under single-scratch conditions but also during reciprocal scratching. Notably, the friction coefficient of the wax-coated surface exhibited large fluctuations at medium and high contact pressures with increasing sliding time, which may be related to the gradual penetration of the coating into the β-HMX surface and thus altered the friction mechanism. In addition, the frictional work-heat conversion rate of the wax-coated β-HMX surface increased from ~19% to ~30% and increased with increasing number of sliding cycles under specific conditions until the contact pressure became too high and the lubricating effect of the wax layer failed. This finding emphasizes the protective role of the wax layer in the early stages of friction and its limitations under extreme friction conditions.

Acknowledgements

The project was supported by the National Natural Science Foundation of China (Nos. 52575239, 12472372, and 12272051), the Science Challenge Project (No. TZ20250001), the Tribology Science Fund of the State Key Laboratory of Tribology in Advanced Equipment (No. SKLTKF22A01), and the funding from the Sichuan Science and Technology Program (Nos. 2024NSFSC0147 and 2024NSFTD0019).

Declaration of competing interest

The authors have no competing interests to declare that are relevant to the content of this article.

Electronic Supplementary Material

Supplementary material is available in the online version of this article at https://doi.org/10.26599/FRICT.2025.9441063.

References

[1] Lai Q, Pei L, Fei T, Yin P, Pang S P, Shreeve J M. Size-matched hydrogen bonded hydroxylammonium frameworks for regulation of energetic materials. *Nat Commun* **13**(1): 6937 (2022)

[2] Zhang W Q, Zhang J H, Deng M C, Qi X J, Nie F D, Zhang Q H. A promising high-energy-density material. *Nat Commun* **8**(1): 181 (2017)

[3] Badgujar D M, Talawar M B, Asthana S N, Mahulikar P P. Advances

in science and technology of modern energetic materials: An overview. *J Hazard Mater* **151**(2–3): 289–305 (2008)
[4] Zeman S, Jungová M. Sensitivity and performance of energetic materials. *Propell Explos Pyrot* **41**(3): 426–451 (2016)
[5] Cao Z M, He C L, Zong W J, Huang J H, Wei Z Y. Modeling of heat partitioning and temperature rise at the tool-chip interface in diamond turning of the PBX surrogate. *J Manuf Process* **87**: 160–167 (2023)
[6] Perry W L, Gunderson J A, Balkey M M, Dickson P M. Impact-induced friction ignition of an explosive: Infrared observations and modeling. *J Appl Phys* **108**(8): 084902 (2010)
[7] Parker G R, Holmes M D, Heatwole E M, Broilo R M, Pederson M N, Dickson P M. Direct observation of frictional ignition in dropped HMX-based polymer-bonded explosives. *Combust Flame* **221**: 180–193 (2020)
[8] He H, Zhu P, Liu R, Cao Z, Cai C, Yu J, Yin Y. Research advances and prospective on tribological properties of energetic materials. *Tribology* **43**(10): 1222–1238 (2023) (in Chinese)
[9] Kazumi T, Hara K, Yu Y H, Yamato Y, Takahori T, Shimizu Y, Yoshida T. Safety aspect of a non-azide propellant for automotive airbag inflators. *J Energ Mater* **14**(2): 81–95 (1996)
[10] Duarte C A, Grilli N, Koslowski M. Effect of initial damage variability on hot-spot nucleation in energetic materials. *J Appl Phys* **124**(2): 025104 (2018)
[11] Andersen W H. Role of the friction coefficient in the frictional heating ignition of explosives. *Propell Explos Pyrot* **6**(1): 17–23 (1981)
[12] Zhong K, Bu R P, Jiao F B, Liu G R, Zhang C Y. Toward the defect engineering of energetic materials: A review of the effect of crystal defects on the sensitivity. *Chem Eng J* **429**: 132310 (2022)
[13] Czerski H, Proud W G. Relationship between the morphology of granular cyclotrimethylene-trinitramine and its shock sensitivity. *J Appl Phys* **102**(11): 113515 (2007)
[14] Van der Heijden A E D M, Creyghton Y L M, van de Peppel R J E, Abadjieva E. Modification and characterization of (energetic) nanomaterials. *J Phys Chem Solids* **71**(2): 59–63 (2010)
[15] Huang B B, Xue Z H, Fu X L, Yan Q L. Advanced crystalline energetic materials modified by coating/intercalation techniques. *Chem Eng J* **417**: 128044 (2021)
[16] Cowey K, Day S, Fryer R. Examination of wax-coated RDX by scanning electron microscopy and X-ray photoelectron spectroscopy. *Propell Explos Pyrot* **10**(3): 61–64 (1985)
[17] He G S, Yang Z J, Zhou X Y, Zhang J H, Pan L P, Liu S J. Polymer bonded explosives (PBXs) with reduced thermal stress and sensitivity by thermal conductivity enhancement with graphene nanoplatelets. *Compos Sci Technol* **131**: 22–31 (2016)
[18] Li N, Zhang Y S, Guo R, Yang J J, Zhang X Y, Wang X. Effect of stearic acid coating on the explosion characteristics of aluminum dust. *Fuel* **320**: 123880 (2022)
[19] Xiao L Q, Zhao Y, Fu X L, Xie W X, Fan X Z. Mechanical sensitivity reduction of energetic materials by using carbon nanomaterials. *J Phys Conf Ser* **2478**(3): 032010 (2023)
[20] An C W, Guo X D, Song X L, Wang Y, Li F S. Preparation and safety of well-dispersed RDX particles coated with cured HTPB. *J Energ Mater* **27**(2): 118–132 (2009)
[21] Zhao J, Li Q Z, Li S X, Li S C, Chen G Y, Liu X H, He Y Y, Luo J B. Influence of a carbon-based tribofilm induced by the friction temperature on the tribological properties of impregnated graphite sliding against a cemented carbide. *Friction* **9**(4): 686–696 (2021)
[22] Xiao J K, Wu Y Q, Zhang W, Chen J, Zhang C. Friction of metal-matrix self-lubricating composites: Relationships among lubricant content, lubricating film coverage, and friction coefficient. *Friction* **8**(3): 517–530 (2020)
[23] Yin Y, Li H T, Cao Z H, Li B H, Li Q S, He H T, Yu J X. Crystallographic orientation dependence on nanoscale friction behavior of energetic β-HMX crystal. *Friction* **11**(12): 2264–2277 (2023)
[24] Li H T, Sun J, Sui H L, Chai C G, Li B H, Yu J X, He H T, Yin Y. Influencing mechanisms of a wax layer on the micro-friction behavior of the β-HMX crystal surface. *Energ Mater Front* **3**(4): 248–256 (2022)
[25] Philip J, Hess P, Feygelson T, Butler J E, Chattopadhyay S, Chen K H, Chen L C. Elastic, mechanical, and thermal properties of nanocrystalline diamond films. *J Appl Phys* **93**(4): 2164–2171 (2003)
[26] Perriot R, Cawkwell M J. Thermal conductivity tensor of β-1,3,5,7-tetranitro-1,3,5,7-tetrazoctane (β-HMX) as a function of pressure and temperature. *J Appl Phys* **130**(14): 145106 (2021)
[27] Yuan J M, Qin Y, Peng H Z, Xia T, Liu J Y, Zhao W, Sun H, Liu Y. Experiment and numerical simulation on friction ignition response of HMX-based cast PBX explosive. *Crystals* **13**(4): 671 (2023)
[28] Xiao X M, Yin Y, Bao J S, Lu L J, Feng X J. Review on the friction and wear of brake materials. *Adv Mech Eng* **8**(5): 1687814016647300 (2016)
[29] Rowe K G, Bennett A I, Krick B A, Gregory Sawyer W. *In situ* thermal measurements of sliding contacts. *Tribol Int* **62**: 208–214 (2013)
[30] Dai H Y, Fan J C, Wu S N, Yu Y Q, Liu D, Hu Z B. Experimental study on ignition mechanisms of wet granulation sulfur caused by friction. *J Hazard Mater* **344**: 480–489 (2018)
[31] Li G C, Qu Y Y, Liu R, Duan H J, Yu J X, He H T, Yin Y. Friction-induced temperature rise at energetic β-HMX crystal interfaces: Part I. Role of contact pressure and speed under dry sliding friction. *Tribol Int* **199**: 110006 (2024)
[32] Sui Z L, Sun X Y, Liang W T, Dai R C, Wang Z P, Huang S L, Zheng X X, Zhang Z M, Wu Q. Phase confirmation and equation of state of β-HMX under 40 GPa. *J Phys Chem C* **123**(50): 30121–30128 (2019)
[33] Gao H, Wang Q H, Ke X, Liu J, Hao G Z, Xiao L, Chen T, Jiang W, Liu Q E. Preparation and characterization of an ultrafine HMX/NQ co-crystal by vacuum freeze drying method. *RSC Adv* **7**(73): 46229–46235 (2017)
[34] Du X F, Wang S J, Wang P, Gu Q, Xin J, Zhang Z X, Wang J, Yao C P. Characterization of paraffin-waxed apples by Raman spectroscopy. *Anal Lett* **53**(2): 217–227 (2020)
[35] Wu W, Shao T M, Chen G M. Influence of groove surface texture on temperature rise under dry sliding friction. *Sci China Technol Sc* **59**(2): 183–190 (2016)
[36] Shakhvorostov D, Pöhlmann K, Scherge M. An energetic approach to friction, wear and temperature. *Wear* **257**(1–2): 124–130 (2004)
[37] Qin J G, Chen R, Wen X J, Lin Y L, Liang M Z, Lu F Y. Mechanical behaviour of dual-phase high-strength steel under high strain rate tensile loading. *Mater Sci Eng A* **586**: 62–70 (2013)
[38] Tarver C M, Tran T D. Thermal decomposition models for HMX-based plastic bonded explosives. *Combust Flame* **137**(1–2): 50–62 (2004)
[39] Hao G C, Liu Z Q. The heat partition into cutting tool at tool-chip contact interface during cutting process: A review. *Int J Adv Manuf Tech* **108**(1): 393–411 (2020)
[40] Zhao J F, Liu Z Q, Wang B, Hu J R, Wan Y. Tool coating effects on cutting temperature during metal cutting processes: Comprehensive review and future research directions. *Mech Syst Signal Pr* **150**: 107302 (2021)
[41] Watkins S A, Lee R J, Hewitt A T, Mankowski J, Brinkman J, Dickens J, Neuber A A. An investigation into the surface skidding response of PBX 9501 and PBX 9502. *Propell Explos Pyrot* **47**(7): e202200010 (2022)
[42] Habchi W, Bair S. The role of the thermal conductivity of steel in quantitative elastohydrodynamic friction. *Tribol Int* **142**: 105970 (2020)
[43] Jin B, Peng R F, Chu S J, Huang Y M, Wang R. Study of the desensitizing effect of different [60] fullerene crystals on cyclotetramethylenetetranitramine (HMX). *Propell Explos Pyrot* **33**(6): 454–458 (2008)
[44] Hua C, Zhang P J, Lu X J, Huang M, Dai B, Fu H. Research on the size of defects inside RDX/HMX crystal and shock sensitivity. *Propell Explos Pyrot* **38**(6): 775–780 (2013)

[45] Radacsi N, Bouma R H B, Krabbendam-la Haye E L M, Ter Horst J H, Stankiewicz A I, Van der Heijden A E D M. On the reliability of sensitivity test methods for submicrometer-sized RDX and HMX particles. *Propell Explos Pyrot* **38**(6): 761–769 (2013)
[46] Browning R V. Microstructural model of mechanical initiation of energetic materials. *AIP Conf Proc* **370**: 405–408 (1996)
[47] Liu R, Chen P W, Zhang X T. Effect of continuous damage accumulation on ignition of HMX-based polymer bonded explosives under low-velocity impact. *Propell Explos Pyrot* **45**(12): 1908–1919 (2020)
[48] Liu R, Wang X J, Chen P W, Kang G, Zhu S P, Guo Y S. The role of tension–compression asymmetrical microcrack evolution in the ignition of polymer-bonded explosives under low-velocity impact. *J Appl Phys* **129**(17): 175108 (2021)
[49] Li X, Liu Y Z, Sun Y. Dynamic mechanical damage and non-shock initiation of a new polymer bonded explosive during penetration. *Polymers* **12**(6): 1342 (2020)
[50] Yang K, Wu Y Q, Huang F L. Damage and hotspot formation simulation for impact-shear loaded PBXs using combined microcrack and microvoid model. *Eur J Mech A—Solid* **80**: 103924 (2020)
[51] Talamadupula K K, Povolny S J, Prakash N, Seidel G D. Mesoscale strain and damage sensing in nanocomposite bonded energetic materials under low velocity impact with frictional heating via peridynamics. *Modell Simul Mater Sc* **28**(8): 085011 (2020)
[52] Duan H Z, Wu Y Q, Hou X, Yang K, Maimaitituersun W, Huang F L. Ignition response of NEPE-based propellants under drop weight through experiments and numerical simulation. *J Energ Mater* **43**(2): 247–268 (2025)
[53] Duan H Z, Wu Y Q, Yang K, Huang F L. Numerical simulation of drop weight impact sensitivity evaluation criteria for pressed PBXs. *Def Technol* **19**: 76–90 (2023)
[54] Hunt E M, Malcolm S, Pantoya M L, Davis F. Impact ignition of nano and micron composite energetic materials. *Int J Impact Eng* **36**(6): 842–846 (2009)
[55] Duan H J, Li G C, Liu R, Zhang H, Yu J X, Yin Y, He H T. Friction-induced temperature rise at energetic β-HMX crystal interfaces: Part II. Simulation of HMX rough surface under dry friction conditions. *Tribol Int* **197**: 109833 (2024)
[56] Li J L, Lu F Y, Qin J G, Chen R, Zhao P D, Lan L G, Jing S M. Effects of temperature and strain rate on the dynamic responses of three polymer-bonded explosives. *J Strain Anal Eng* **47**(2): 104–112 (2012)

Hongtu He received his B.S. degree and Ph.D. degree from Southwest Jiaotong University, China, in 2010 and 2015, respectively. From 2018 to 2020, he worked as a visiting professor at Pennsylvania State University, USA. He is now working as a professor at Southwest University of Science and Technology. His research interests include microtribology, glass surface science, mechanochemistry, and energetic materials.

Ying Yin is an associate professor at the Institute of Chemical Materials, the China Academy of Engineering Physics. He received his Ph.D. degree in aerospace science and technology from the Harbin Institute of Technology, China, in 2017. His research areas include ammunition aging and environmental adaptability and surface and interface analysis of advanced energetic materials.